Assessment of Subgrid-Scale Model Effects on Large Eddy Simulation of a Back-Step Combustor

Weilin Zeng[1], Konstantina Vogiatzaki[2], Kai Hong Luo[1]* and Salvador Navarro-Martinez[3]
[1] Department of Mechanical Engineering, University College London, Torrington Place, London WC1E 7JE, UK
[2] Advanced engineering Center, University of Brighton, Lewes Road, Brighton, BN2 4AT, UK
[3] Department of Mechanical Engineering, Imperial College, South Kensington Campus, London SW7 2AZ, UK

Abstract

Much progress has been made in large-eddy simulation (LES) of turbulent combustion in the last two decades, but a robust and cost-effective LES formulation is still lacking for turbulent combustion in practical configurations. In this paper, we present an assessment of different sgs models and the no sgs approach within the context of LES of a backward step combustor. Overall, the dynamic one equation eddy model behaves better than the WALE and one equation eddy models, in both reproducing main features and statistical quantities of the non-reactive and reactive flow fields. Increasing grid resolution does not necessarily improve the predictions. The results are largely dependent on whether the local flow is turbulence or combustion dominated. This implies that along with an adaptive grid refinement, an adaptive combustion model strategy is needed. In combustion simulation, applying only the first term in the series model is insufficient to well predict the dominating features and statistical quantities of the reacting flows. Thus, we suggest as future work the introduction of additional adaptive terms that will control the variance.

NOMENCLATURE

ν - Kinematic viscosity (m^2/s)
u_i - Velocity opponent in i direction (m/s)
ρ - Density (kg/m^3)
p - Pressure (N/m^2)
k_{sgs} - Subgrid kinetic energy
h_s - Sensible enthalpy (kJ/kg)
Y_i - Mass fraction
μ - Dynamic viscosity ($N*s/m^2$), $\mu = \nu*\rho$
$\dot{\omega}$ - Chemical source term

Introduction

Turbulent reacting flows involve a wide range of time and length scales depending on the specific combustor design as well as the operating conditions [1]. Large Eddy Simulation (LES) represents one of the most promising techniques for the evaluation of the dynamics of turbulent structures characterising propulsion systems. In LES a spatially localized filter is applied to a single realization of the studied flow. Resulting from this spatial filtering is a separation between large scales (greater than the filter size and thus resolved on the grid) and scales smaller than the filter size, which requires modelling. Although the theoretical potential of the method to predict transient phenomena is already widely accepted, in reality it does not guarantee that it is applicable. A major limitation of LES when applied to industrial configurations is the uncertainties introduced by the subgrid-scale (sgs) models. These models, depending on the assumptions they are derived, have limitaitons in the physiscs they can represent. Also some models do not have the correct limiting behaviour as the grid size approached Kolmogorov scale. Another problem of LES is the high computational overload. In most LES studies presented in the literature this results from the higher grid resolution and smaller time-steps in comparison to RANS as well as the use of sgs turbulent combustion models over the whole computational domain, even in areas that not much information in reality lies "below" the grid size. Although the issue of overload resulting from the grid resolution has been addressed by adaptive grid methodologies, less tried are adaptive turbulent combustion models. Apart from adding to the computational cost, non-adaptive models also lead to wrong predictions in some areas. It should be noted that for example most turbulence models are derived based on the idea of enforcing energy dissipation from large scales to smaller ones. However, in more laminarised areas of the flow the assumption of turbulence cascade fails and the models overestimate the local energy dissipation.

In this work we present an investigation of a lean premixed flame in a backward-facing step combustor, using LES with different sgs models. In order to assess the sgs models we first identify the areas in which subgrid scales have the greatest impact within the configuration. This is done with a combination of local scales calculation and sensitivity analysis of the model closures. We distinguish flow regions more affected by turbulence alone and regions that the combined effect of chemistry-turbulence interaction is dominant. Initially, different sgs models, as well as a "no-model approach", are applied on unresolved Reynolds stresses in two different grid resolutions under non-reactive conditions. Subsequently, combustion is activated and the effect of the sgs combustion sclaes is assessed.

Combustor Set-up

The experimental data in this paper are from a backward-facing step combustor, whose schematic is

* Corresponding author: k.luo@ucl.ac.uk

depicted in Fig. 1. The data were obtained at Reacting Gas Dynamics of MIT, and a number of papers have already been published [2-4]. The combustor consists of a rectangular stainless steel duct with a cross section 0.040 m high and 0.160 m wide. The air inlet is choked. At a location 0.45 m downstream from the choke plate, a 0.15 m long ramp reduces the channel height from 0.040 m to 0.020 m, followed by a 0.4 m long constant area section that ends with a sudden expansion back to 0.040 m. The step height is 0.020 m. The overall length of the combustor is 5 m. The exhaust exits to a trench with a large cross sectional area. Quartz viewing windows 0.4 m wide is installed in the vicinity of the step, providing optical access. Planar velocity fields and flame surface topology were obtained using phase-locked particle image velocimetry (PIV) and the measurements were processed using the LaVision DaVis 7.2 software. More details for the experimental set-up can be found in [4]. To investigate the stability characteristics of the combustor, both isothermal and combustion simulations were performed, at an equivalence ratio of the fuel air mixture of C3H8 near to the lean blow-off limit (φ = 0.63). The key quantities relevant to the configuration are described in Table 1.

Table 1. Parameters for the combustor configuration [4]

Parameter	Expression	Value
Step Height (Characteristic Length)	h_s	20mm
Integral Length Scale	$L_I (=h_s)$	20mm
Bulk Inlet Velocity (Characteristic Flow Velocity)	U_{sh}	5.2sm/s
Macroscopic Reynolds Number	Re_{sh}	6,500
Inlet Temperature	T_s	300K
Nominal Pressure	P	101kPa
Kolmogorov Length Scale	$Re_{sh}^{-3/4}h_s$	27.6um
Cold Flow Filter Width (Pope's Criterion[5])	$\triangle=0.083L_I$	1.66mm
Shear Layer Fluctuation (measured)	$u`$	1m/s
Integral Time Scale	$t_I=h_s/u`$	20ms
Kolmogorov Time Scale	$Re_{sh}^{-1/2}/t_I$	0.25ms
CFL Criterion Time Scale	$C_{max}\triangle x/(U_{sh}+U_{sound})$	2.8us

Numerical Setup

The open source LES code OpenFoam [6] has been used for the simulations presented in this paper. OpenFoam is an unstructured finite-volume code. The density-weighted, filtered compressible Navier-Stokes equations used are as follows:

$$\frac{\partial \bar{\rho}}{\partial t}+\frac{\partial}{\partial x_j}(\overline{\rho u_i})=0 \quad (1)$$

$$\frac{\partial \overline{\rho}\tilde{u}_i}{\partial t}+\frac{\partial(\overline{\rho}\tilde{u}_i\tilde{u}_j)}{\partial x_j}=-\frac{\partial \bar{P}}{\partial x_i}+\frac{\partial}{\partial x_j}[\overline{\tau_{ij}}-(\overline{u_i u_j}-\tilde{u}_i\tilde{u}_j)] \quad (2)$$

$$\frac{\partial \bar{\rho}\tilde{Y}_k}{\partial t}+\frac{\partial}{\partial x_i}\left(\bar{\rho}\tilde{u}_i\tilde{Y}_k\right)=\frac{\partial}{\partial x_j}\left[\overline{V_{k,s}Y_k}-\bar{\rho}\left(\widetilde{u_iY_k}-\tilde{u}_i\tilde{Y}_k\right)\right]+\overline{\dot{\omega}_k} \quad (3)$$

$$\frac{\partial \bar{\rho}\tilde{h}_s}{\partial t}+\frac{\partial}{\partial x_j}\left(\bar{\rho}\tilde{u}_j\tilde{h}_s\right)=\frac{\overline{Dp}}{Dt}+\frac{\partial}{\partial x_j}\left[\overline{\lambda\frac{\partial T}{\partial x_j}}-\bar{\rho}\left(\widetilde{u_ih_s}-\tilde{u}_i\tilde{h}_s\right)\right]+\overline{\tau_{ij}\frac{\partial u_i}{\partial x_j}}-\frac{\partial}{\partial x_j}\left(\rho\sum_{s=1}^{N}\overline{V_{s,j}Y_sh_{s,s}}\right)+\overline{\dot{\omega}_T} \quad (4)$$

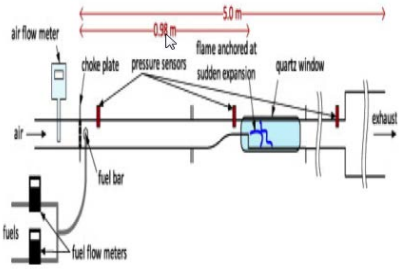

a)

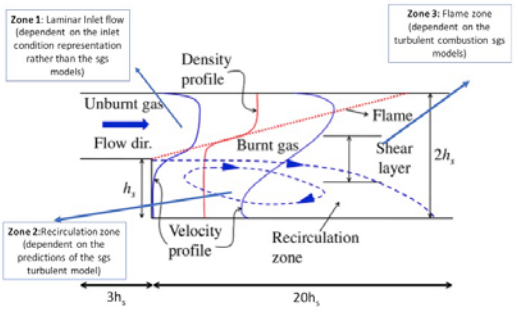

b)

Figure 1: a) Experimental set-up of the backward facing step combustor [4] b) Schematic of the combustor simulation geometry and flow features

Sgs modelling in the context of LES in practice is the closure of two terms in the above equations: the sgs stress tensor (τ_{ij}) and the filtered reaction rate ($\bar{\dot{\omega}}$). These equations are solved as a group and the turbulence chemistry interaction is a highly non-linear process, which makes it challenging to identify the effect of each individual term. In our analysis we first look into the accuracy of the predictions of various turbulence models for a non-reactive case. This part of the analysis will help us to a) to identify different flow areas that are dominated by different characteristics (laminar region, recirculation zone, turbulent/combusting flow, see Fig. 1b b) to evaluate the connection between local scales and grid resolution c) to evaluate the performance of the turbulence modelling at the various zones.

Then, we proceed to the analysis of the reaction case. For this case we assume that $\overline{\dot{\omega}(\xi)}=\dot{\omega}(\bar{\xi})$ based on a Taylor Series analysis as will be explained in the following paragraphs. In this way, in reactive simulations although we use model for turbulence we do not explicitly model turbulence chemistry interaction at the sgs scale but only at the grid scale level. Diversion of the experimental data is expected, especially in the zones that our non-reactive simulations indicated the importance of turbulence as more pronounced. We use this approach as a guide to quantify "how much" information the sgs scales carry at various zones. This will guide us for the "adaptive" modelling of the rest of Taylor Series model terms in the future.

Turbulence Modelling

There are several models for the sgs component τ_{ij} in Eq. (2). Two popular types of models are: a)

algebraic eddy viscosity models in which the stress tensor is related to the resolved strain rate tensor S_{ij} by means of a scalar eddy viscosity given by an algebraic equation (for example Wall-Adapting Local Eddy-viscosity model model [7]; and b) one-equation eddy viscosity models (simple or dynamic formulations). Both model groups are based on the Boussinesq hypothesis associating the sgs stress tensor with a sgs turbulent viscosity ν_τ. The idea is that the momentum transfer caused by turbulent eddies can be modelled with an eddy viscosity in the same way that the momentum transfer caused by the molecular motion in a gas can be described by a molecular viscosity. Here we assess three popular models along with a "no sgs" approach:

- The one equation eddy model (denoted as "OneEqEddy"), using a modelled balance equation to simulate the behaviour of the sgs turbulence intensity (k_{sgs}) as follows,

$$\frac{\partial k_{\mathrm{SGS}}}{\partial t}+\tilde{u}_i\frac{\partial k_{\mathrm{SGS}}}{\partial x_i}=-\tau_{ij}\frac{\partial \tilde{u}_i}{\partial x_j}-\varepsilon_{\mathrm{SGS}}+\frac{\partial}{\partial x_i}\left(\nu_T\frac{\partial k_{\mathrm{SGS}}}{\partial x_i}\right). \quad (5)$$

where

$$\nu_T=C_\tau\bar{\Delta}k_{\mathrm{SGS}}^{1/2}, \qquad \varepsilon_{\mathrm{SGS}}=C_e\frac{k_{\mathrm{SGS}}^{3/2}}{\bar{\Delta}}$$

Using k_{SGS}, the sgs stress tensor is modelled as:

$$\tau_{ij}=-2C_\tau\bar{\Delta}k_{\mathrm{SGS}}^{1/2}\bar{S}_{ij}+\frac{2}{3}\delta_{ij}k_{\mathrm{SGS}} \quad (6)$$

- The algebraic WALE model where the eddy viscosity is modelled as follows:

$$\mu_T=\rho\Delta^2\frac{(S_{ij}^dS_{ij}^d)(3/2)}{(\bar{S}_{ij}\bar{S}_{ij})^{5/2}+(S_{ij}^dS_{ij}^d)^{5/4}} \quad (7)$$

with

$$\Delta=C_wV^{1/3}$$

$$S_{ij}^d=\frac{1}{2}(\tilde{g}_{ij}^2+\tilde{g}_{ji}^2)-\frac{1}{3}\delta_{ij}\tilde{g}_{kk}^2 \qquad \tilde{g}_{ij}=\frac{\partial\tilde{u}_i}{\partial x_j}$$

The main feature of the WALE model is that the sgs viscosity is dynamically computed with the square of the velocity gradient tensor rather than the resolved strain rate used in Smagorinsky-type models. This velocity tensor can not only account for the effects of both strain and rotation rate of the smallest resolved turbulence fluctuations, but also recover the proper near-wall scaling for the eddy viscosity without requiring dynamic procedure. Moreover, the WALE model is invariant to any coordinate translation or rotation and no test-filtering operation is needed, it is therefore well suitable for LES in complex geometries [7].

- The dynamic one equation subgrid model [1] (denoted as "DynOneEqEddy"), which derives the SGS kinetic energy by solving the same transport equation as the simple one equation model (see Eq. (5)). The difference is that dynamic procedures are employed to evaluate Cτ and Cε using a test filter field that is constructed from the grid-scale field by applying a test filter characterized by Δ`(typically, Δ` =2Δ [8])

Analysis of results has shown that the dynamic one equation model is Galilean-invariant and satisfies well [8] the reliability conditions given by Schumann [9]. From a computational standpoint, the cost of the present dynamic procedure is not significant (about the same as that for the dynamic model by Germano et al. [10]) due to its simplicity. The additional computational cost is primarily due to the inclusion of a transport equation for k_{SGS} which is the same as the case on the non-dynamic model. The justification for this extra computational cost is that this approach has the aforementioned advantage over algebraic models (such as WALE model) since the equilibrium assumption is not required. Furthermore, k_{SGS} provides a more accurate estimate for the SGS velocity scale [11]. For completeness the "no sgs" approach is also tested, where sgs stress tensor is eliminated in the filtered momentum equation, so that non-reacting LES simulation can be also seen as a "coarse" DNS.

Combustion Modelling

In Eq. (3), the filtered chemical source term also needs to be modelled. Here, we introduce a new series model to close the filtered source term.

First, we expand the source term in series. For simplicity, the formulation is presented for one species but in reality there are *n* species $Y=[Y_1,\ldots Y_n]$.

$$\dot{\omega}(Y)\approx\dot{\omega}(\bar{Y})+\left.\frac{\partial\omega}{\partial Y}\right|_{Y=\bar{Y}}\delta Y+\frac{1}{2}\left.\frac{\partial^2\dot{\omega}}{\partial Y^2}\right|_{Y=\bar{Y}}(\delta Y)^2+\ldots \quad (8)$$

$$\delta Y=\frac{\partial Y}{\partial x_i}\delta x_i \quad (9)$$

$$\dot{\omega}(Y)=\dot{\omega}(\bar{Y})+\left.\frac{\partial\dot{\omega}}{\partial Y}\right|_{Y=\bar{Y}}\frac{\partial Y}{\partial x_i}\delta x_i+\frac{1}{2}\left.\frac{\partial^2\dot{\omega}}{\partial Y^2}\right|_{Y=\bar{Y}}\left(\frac{\partial Y}{\partial x_i}\right)^2(\delta x_i)^2+TE \quad (10)$$

Then add the filtering operation

$$\overline{\dot{\omega}(Y)}=\overline{\dot{\omega}(\bar{Y})}+\sum\frac{1}{n!}\left.\frac{\partial^n\dot{\omega}}{\partial Y^n}\right|_{Y=\bar{Y}}\overline{\left(\frac{\partial Y}{\partial x_i}\right)^n}M^n \quad (11)$$

$$M^n=\int z^nG(z)dV' \quad (12)$$

$$\overline{\dot{\omega}(Y)}=\overline{\dot{\omega}(\bar{Y})}+\frac{1}{2}\left.\frac{\partial^2\dot{\omega}}{\partial Y^2}\right|_{Y=\bar{Y}}\overline{\left(\frac{\partial Y}{\partial x_i}\frac{\partial Y}{\partial x_j}\right)}\frac{\Delta^2}{12}+TE \quad (13)$$

Now, the filtered source term consists of two terms: first term $\overline{\dot{\omega}(\bar{Y})}$ and $\frac{1}{2}\left.\frac{\partial^2\dot{\omega}}{\partial Y^2}\right|_{Y=\bar{Y}}\overline{\left(\frac{\partial Y}{\partial x_i}\frac{\partial Y}{\partial x_j}\right)}\frac{\Delta^2}{12}$.

In the paper, we only consider the first term, which is equal to a no model approach in order to understand what is the importance of the extra terms. It is anticipated that results will not be perfect but the concept is to try to identify in which areas the problem is more pronounced, understand the physics prevailing these areas and link it to the new model.

Now we try to assess the effect of SGS models on the step combustor simulation, with 2 sets of numerical experiments, non-reacting and reacting. Two grid resolutions are used in x, y and z direcitons: a) 270*120*16, denoted as Medium; b) 350*160*48, denoted as Fine. The simulation time durations are

1.5μs and 1μs for non-reacting simulations, and 1μs and 0.75μs for reacting simulations respectively.

Simulations are performed with periodic boundary conditions in the spanwise direction. At the inlet, Dirichlet conditions are used for all variables except the pressure, for which zero Neumann conditions are specified. At the exit, zero Neumann conditions are specified for all variables except the pressure, for which wave-transmissive conditions are used. No-slip conditions are applied for the flow at the top and bottom walls of the duct, while zero Neumann conditions are specified for the other variables. In order to maintain reasonable computational efficiency, Spalding's wall functions [12] are utilized to resolve the flow features in the wall boundary layer. Numerical computations start from quiescent conditions and the unsteady flow characteristics evolve naturally. To initiate the flame, a high temperature pulse is applied at the inlet section which ignites the fuel; the reacting mixture convects downstream, and eventually stabilizes as a flame in the wake of the step [4]. Averaging is performed over nearly 6 flow-through cycles once the flow is established in the computational domain.

Results and Discussions

Figure 2 shows the comparison of the contours of the averaged axial velocity for different turbulence models at medium grid resolution against the experimental PIV data. All turbulence models, including the no-model approach, predict qualitatively the dominating flow features reasonably well. An almost spherical separation bubble is formed below the step, with its centre located in the zero velocity zone at the corner of the step. An elliptical large secondary recirculation zone is also observed further downstream. All simulations reproduce apparently stronger primary and secondary recirculation zones than those in the experiment. The one equation eddy model shows quite different (in shape and size) primary and secondary recirculation zones from the experimental results. The WALE model predicts an additional small recirculation zone between the primary and secondary eddies close to the wall, which is not evident by the PIV measurements. The dynamic one equation eddy model behaves well in those aspects, while the no model approach is also reproducing reasonably well the main flow features.

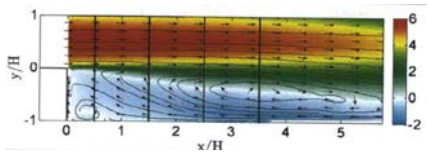

a) PIV Data[4]

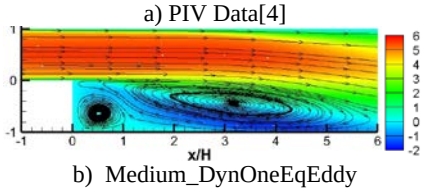

b) Medium_DynOneEqEddy

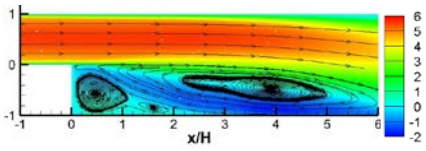

c) Medium_WALE

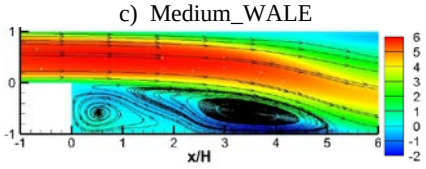

d) Medium_OneEqEddy

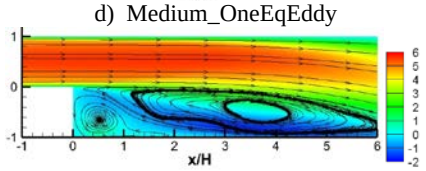

e) Medium_noSgs

Figure 2 Average axial velocity and streamlines

Figure 3 shows the normalised profiles of the average and rms axial velocity at the medium grid resolution. Average results indicate that all models achieve a good agreement with PIV observations of the flow field in the recirculation zones and the shear layer region, except that, one equation eddy model exhibits a larger deviation, due to a poorer reproduction of the recirculation zones shown in Fig. 1. For the rms profiles, although all models predict rather poorly the region below the step, they manifest a reasonable trend. The largest discrepancy from the PIV results appears in the neighbouring region near the upper and lower walls, where a better wall function is needed. Although the dynamic one equation eddy model excels compared with other models, the no model approach still has a good performance. It can be expected that, appropriately matching the inlet fluctuations with PIV results and increasing grid resolution in spanwise direction would improve the accuracy in predicting rms.

To further assess the effect of sgs, Fig. 4 depicts the normalised profiles of the average and rms axial velocity at a finer grid resolution. Results for the average velocity present a good agreement with experimental measurements for all axial locations. As expected, at the fine grid all the models behave similarly, and it can be explained that the grid is fine enough so that sgs models do not play a dominant role. Notably, the one equation eddy model with a fine grid behaves a lot better than at the medium grid resolution. As for the rms profiles, all simulations predict a very good agreement at the upper part (y/H >0), but a rather surprisingly worse accordance near the shear layer and at the lower part of the combustor when compared to the medium grid. Also it is interesting to note that this also happens to the dynamic one equation eddy model, which in theory is the most sophisticated one since it is both locally adaptive due to dynamic procedures and equations based (not algebraic as the WALE). It is believed that this is due to the fact that many existent turbulence models currently used in the literature do not have the correct limiting behaviour when the grid size Δx

tends to 0. They tend to predict a rather turbulent behaviour (higher rms) even in areas with low rms. Looking at the results of both resolutions, we can see that the no sgs-approach is acceptable and this is because there is a natural analogy between the numerical diffusion induced by the grid and the turbulent diffusion imposed by the model.

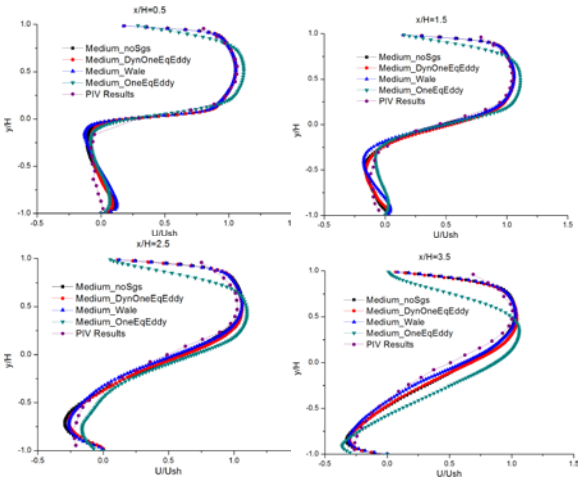

a) Average

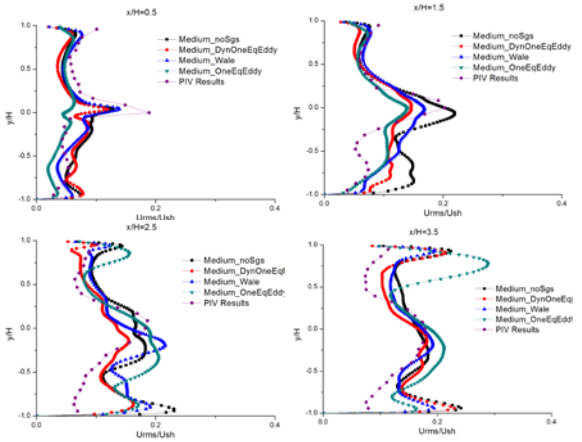

b) RMS

Figure 3 Axial velocity profile

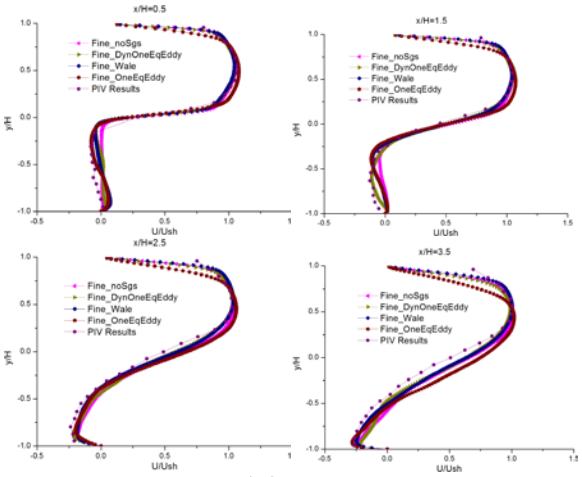

a) Average

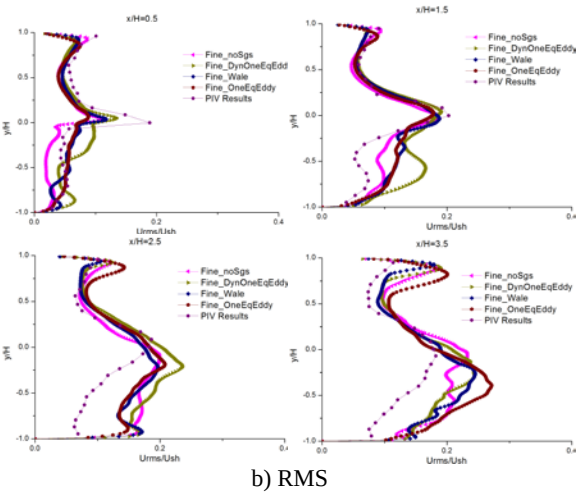

b) RMS

Figure 4 Axial velocity profiles

Figure 5 depicts the comparison of the contours of the averaged axial velocity for reacting simulations at medium and fine grid resolutions and experimental PIV data using Dynamic One Equaiton Model. Regardless of the grid resolution the two simulations fail to reproduce the secondary recirculation zone, and predict a larger primary recirculation zone, compared to the PIV data. This can be attributed to the no model approach applied on the filtered source term and simple one-step propane combustion mechanism used. These predictions indicate that in terms of non-reactive flow fields modelling, for areas dominated by turbulence eddies a relatively fine grid and controlled numerical dissipation can balance the need of a turbulence model. However, this is not sufficeint for reactive cases at least for premixed combustion mode that is dominated by very thin flame fronts.

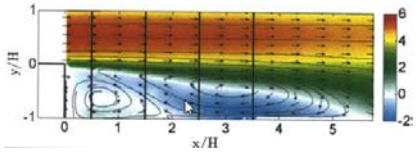

a) PIV Data[4]

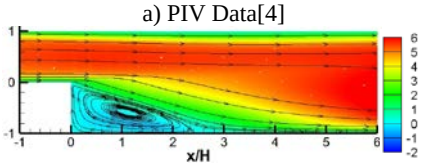

b) Medium grid

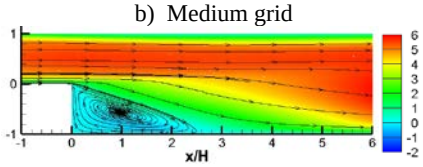

c) Fine grid

Figure 5 Average axial velocity and stream lines for reacting cases

Figure 6 depicts the comparison of the contours of the averaged axial velocity for reacting simulations at medium and fine grid resolutions and experimental PIV data. As to the mean statistics, both simulations achieve a good agreement with experimental data at the upper part of the combustor, but at the lower part where combustion happens and products reside, they

present a large deviation from experiments. These are the zones that the turbulent models also do not behave, however, combustion seems to increase the discrepancy. It also can be seen that when grid resolution is increased, the mean profiles improve slightly. Looking at rms values, fine grid resolution provides results better than medium resolution, especially where x/H >= 1.0. This is different from what we noticed for the non-reactive case, implying that in some cases no-sgs model with fine grid might be a better modelling approach than using a sgs molel without the correct limiting behaviour. It should be noticed that regardless of the previous comment both simulations fail to produce a reasonably good accordance with experiments. Overall, results indicate that a second term is needed to resolve the sgs in the filtered source term, especially for the lower part of the combustor.

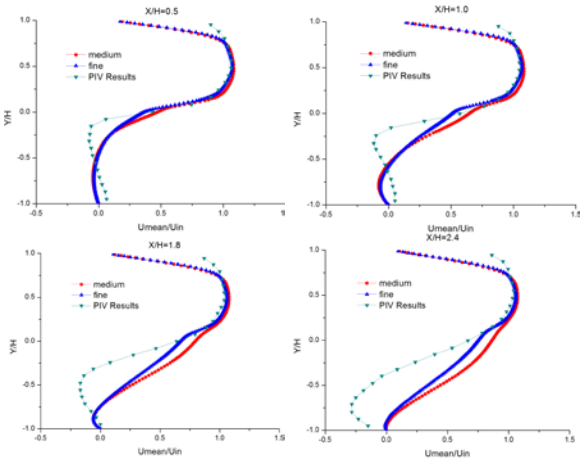

a) Average

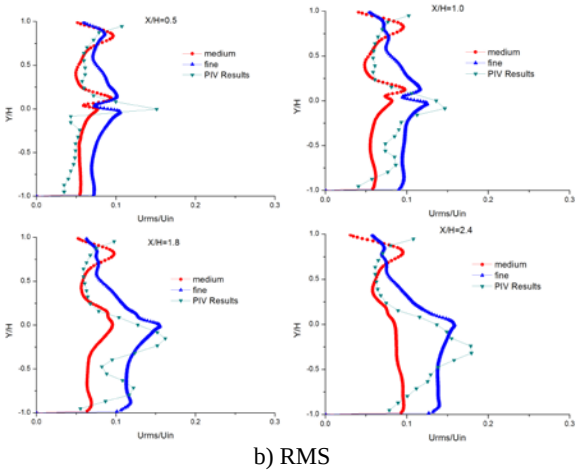

b) RMS

Figure 6 Axial velocity profiles for reacting cases

Conclusions

In this paper, we present an assessment of different sgs models and the no sgs approach within the LES context of a backward step combustor. The dynamic one equation eddy model behaves better than the WALE and one equation eddy models, in both reproducing the main flow features and statistical quantities of the flow field. Increasing grid resolution does not necessarily improve the predictions. The results are largely dependent on whether the local flow is turbulence or combustion dominated. This implies that along with an adaptive grid refinement, an adaptive combustion model is needed. In combustion simulation, applying only the first term in the series model is insufficient to well predict the dominating features and statistical quantities of the reacting flows. Thus, we suggest as future work the introduction of additional adaptive terms that will control the variance.

Acknowledgements

Sponsorship for Weilin Zeng by the China Scholarship Council (CSC) is gratefully acknowledged. The simulations were performed on ARCHER funded under the UK EPSRC project “High Performance Computing Support for United Kingdom Consortium on Turbulent Reacting Flow (UKCTRF)” (Grant No. EP/K024876/1).

References

[1]. Gicquel, L. Y., Staffelbach, G., & Poinsot, T. (2012). Large eddy simulations of gaseous flames in gas turbine combustion chambers. Progress in Energy and Combustion Science, 38(6), 782-817.

[2]. Altay, H. M., Speth, R. L., Hudgins, D. E., & Ghoniem, A. F. (2009). Flame–vortex interaction driven combustion dynamics in a backward-facing step combustor. Combustion and Flame, 156(5), 1111-1125.

[3]. Altay, H. M., Speth, R. L., Hudgins, D. E., & Ghoniem, A. F. (2009). The impact of equivalence ratio oscillations on combustion dynamics in a backward-facing step combustor. Combustion and Flame, 156(11), 2106-2116.

[4]. Kewlani, G. (2014). Large eddy simulations of premixed turbulent flame dynamics: combustion modeling, validation and analysis (Doctoral dissertation, Massachusetts Institute of Technology).

[5]. Pope, S.B., "Turbulent Flows", Cambridge University Press, 2000.

[6]. OpenCFD, OpenFOAM: The Open Source CFD Toolbox, http://www.openfoam.com.

[7]. F. Nicoud and F. Ducros. Subgrid-scale stress modelling based on the square of the velocity gradient tensor. Flow, Turbulence and Combustion, 62(3):183-200，1999.

[8]. M. Germano, U. Piomelli, P. Moin and W.H. Cabot, A dynamic subgrid-scale eddy viscosity model. Phys. Fluids A, 3, 1760–1765 (1991).

[9]. C. Fureby, G. Tabor, H.G. Weller and A.D. Gosman, A comparative study of subgrid scale models in homogeneous isotropic turbulence. Phys. Fluids, 9, 1416–1429 (1997). .

[10]. U. Schumann. Realizability of Reynolds-stress turbulence models. Phys. Fluids, 20, 721–725 (1976).

[11]. Kim W W, Menon S. An unsteady incompressible Navier–Stokes solver for large eddy simulation of turbulent flows. International Journal for Numerical Methods in Fluids, 1999, 31(6): 983-1017.

[12]. Spalding, D.B., 1961. A single formula for the law of the wall. Journal of Applied Mechanics, 28(3), pp.455-458.